Postprint of: Serdiuk I. E., Wera M., Roshal A. D., Sowiński P., Zadykowicz B., Błażejowski J., Tautomerism, structure and properties of 1,1′,1″-(2,4,6-trihydroxybenzene-1,3,5-triyl)triethanone, Tetrahedron Letters, Vol. 52, Iss. 21 (2011), pp. 2737-2740, DOI: 10.1016/j.tetlet.2011.03.087



# Tautomerism, structure and properties of 1,1',1''-(2,4,6-trihydroxybenzene-1,3,5-triyl)triethanone

Ilia E. Serdiuk[a], Michał Wera[b], Alexander D. Roshal[a], Paweł Sowiński[c], Beata Zadykowicz[b], Jerzy Błażejowski[b,*]

[a] *Institute of Chemistry, V. N. Karazin National University, Svoboda 4, Kharkiv 61077, Ukraine*

[b] *Faculty of Chemistry, University of Gdańsk, J. Sobieskiego 18, Gdańsk 80-952, Poland*

[c] *Faculty of Chemistry, Gdańsk University of Technology, G. Narutowicza 11/12, Gdańsk 80-233, Poland*

## ABSTRACT

According to computational predictions 1,1',1''-(2,4,6-trihydroxybenzene-1,3,5-triyl)triethanone (triacetylphloroglucinol) (TTT, form **a**) can exist in five tautomeric forms, among which 2,4,6-tris(1-hydroxyethylidene)-1,3,5-cyclohexanetrione (form **e**) exhibits thermodynamic stability comparable to that of form **a**. X-ray investigations reveal that the compound exists in form **a** in the crystalline solid phase. Analysis of the arrangement of atoms involved in the three intramolecular H-bonds, responsible for the stabilization of tautomer **a** by 55.4 kcal/mol, suggests that there could be fast H atom (proton) transfer within the hydrogen bonds, bringing about transformation of **a** into **e** and *vice versa*. Such an effect could explain the unique behaviour and spectral properties of TTT in solutions.

*Keywords:* Triacetylphloroglucinol, Tautomerism, Structure, Spectral properties

* Corresponding author. Tel.: +48 58 5235331; fax: +48 58 5235464 (J. Błażejowski); *e-mail address:* bla@chem.univ.gda.pl (J. Błażejowski).

Benzene-1,3,5-triol (phloroglucinol) (BT) can be quite easily substituted with one to three –COH or –COR (R – alkyl) groups, forming derivatives with interesting features.[1–6] Motifs of formylated or acylated BT have been found in naturally occurring polyphenols, their polymers and oligomers.[2,6–10] Phloroglucinol and its derivatives appear to be convenient substrates for the synthesis of biologically active compounds, such as analogues of natural flavonoids, drugs, cosmetics or substances exhibiting features of optical switches.[2,6,10–12] The unique structure, properties and reactivity of these derivatives, a representative of which is 1,1',1''-(2,4,6-trihydroxybenzene-1,3,5-triyl)triethanone (TTT), emerge from keto-enol tautomerism (Figure 1) involving the benzene ring and the –OH and –CO– groups responsible for the chemical properties and reactivity of these compounds.[13–15] Despite numerous studies, the structure and properties of TTT, in which three tautomeric centres occur, are still not fully understood.[3,4,6,10] This paper focuses on the tautomerism and the structural and physicochemical properties of this compound.

TTT can occur in five tautomeric forms as shown in Figure 1. Three types of keto/enol tautomeric equilibria are reflected in these forms (Figure 2): **I** (aromatic hydroxy/alicyclic carbonyl), **II** (aromatic–aliphatic keto/aromatic–aliphatic enol) and **III** (aromatic hydroxy–aliphatic keto/alicyclic–carbonyl, alicyclic enol). Various motifs of the tautomers illustrated in Figure 2 can be found in numerous chemical systems.[6–10,16,17] The stabilities of forms **a**, **b**, and **e** should be greater than those of **c** and **d**, since the former consist of aromatic and/or double bond conjugated systems. Further, forms **a**, **b**, **d**, and **e** should be stabilized by intramolecular H-bonds. It emerges from the above discussion that forms **a**, **b** and **e** may be expected to be more stable than **c** and **d**. However, constants reflecting the equilibria depicted by **I** and **II** in the aqueous phase (Figure 2) suggest that form **a** should prevail over the other tautomers.[14,18]

To acquire more information on the stability of TTT tautomers (Figure 1) and the entities depicted in Figure 2, we carried out unconstrained geometry optimization at the MP2 level[19] using the cc-pVDZ basis set[20,21] and the Gaussian 03 program package,[22] with and without the influence of the solvent; in the former case the Polarized Continuum Model (PCM) was applied (UHF radii were used to obtain the molecular cavity).[23,24] The optimized structures are shown in Figure 1S (Supplementary material) and selected thermodynamic characteristics in Table 1. The most stable tautomer is predicted to be **a**, while next in order of stability is tautomer **e**. However, its amount in equilibrium conditions would be of the order of 2.5 mol% in methanol. The other tautomers cannot be expected to be present in measurable

amounts under these conditions. In the gaseous phase form **a** should predominate (the predicted molar ratio of **e**/**a** is less than $4.2\times10^{-5}$).

The stability of tautomer **a**, as of tautomers **b**, **d** and **e**, is substantially enhanced by three intramolecular H-bonds. To evaluate the contribution of these bonds to this stability, the structure of molecule **a'** in which such bonds do not occur (the initial structure was modelled by turning all the –OH groups through 180º relative to those in **a**) was optimized (this is illustrated in Figure 1S, Supplementary material). It appears that [at the MP2/cc-pVDZ(PCM–methanol) level of theory] the free energy of **a'** is 55.4 kcal/mol higher than that of **a** (in the gaseous phase this difference is equal to 56.1 kcal/mol). Since the molecule investigated exhibits $C_{3v}$ symmetry, one can assume that 1/3 of the free energy difference between **a'** and **a** accounts for the thermodynamic stabilization brought about by a single H-bond. Quite high values of the latter quantity, equal to 18.5 kcal/mol in the methanolic, and 18.7 kcal/mol in the gaseous phase, implies that the intramolecular H-bonds are quite strong.

To check how well the applied approach predicts the behaviour of this group of tautomers, we calculated constants for the equilibria depicted as **I**, **II** and **III** in Figure 2 in the aqueous phase at the MP2/cc-pVDZ(PCM–water) level of theory. The values obtained for **I**, $1.10\times10^{-6}$ (experimental in water, $6\times10^{-4}$);[14] **II**, $1.91\times10^{-11}$ (experimental in water, $1.3\times10^{-8}$);[18] and **III**, $5.04\times10^{-19}$, demonstrate trends similar to those found experimentally. This implies that theory provides a sound prediction of the relative stabilities of TTT tautomers.

Tautomers **a** and **e** exhibit similar arrangements of atoms in their molecules; the former can be transformed into the latter by H-atom transfer from –OH to –CO–. As forms **a** and **e** should have different structural features, we determined the structure of TTT crystallized from methanol. The details of the experimental procedure and refinement are given in the Supplementary material. The molecular structure of the compound is presented in Figure 3, and the arrangement of molecules in the crystal together with intra- and intermolecular interactions in Figures 3 and 4 (also in the Supplementary material).[25,26] All the C and O atoms of the molecules remain in plane in the crystal and in the liquid phase of **a** and **e** (Table 2). This molecular structure is stabilized by three intramolecular H-bonds that can occur in both tautomers. The structure of TTT in the crystalline solid phase is similar to that of BT, although the C–O bonds are shorter in the former compound.[27] Comparing the lengths of the C=O and C–C (ring–acetyl) bonds, the former are longer and the latter shorter in TTT than in acetophenone (1-phenylethanone).[28] Some similarities can be found in the structure of TTT and 1-(2,4,6-trihydroxyphenyl)ethanone involved in crystalline assemblies.[29] It is also worth mentioning that the average length of the C–C (ring) bonds is evidently higher in crystalline

TTT (Table 2) than in benzene.[30] This comparison indicates that the molecular structure of crystalline TTT lies somewhere between the structures of the related compounds, mentioned above. Thorough analysis of the geometry of the molecules and the H-bonds (Table 2) leaves the impression that the experimentally determined one is closer to that predicted for tautomer **a** than **e**. This observation is endorsed by the data in Table 4S (Supplementary material), which demonstrates that the bond lengths predicted at the MP2/cc-pVDZ(PCM–methanol) level for **a** compare better with the X-ray bond lengths than those of **e** [the similarity criterion based on the average value of the relative differences between X-ray and predicted (MP2) bond lengths was used to judge how far the molecular structures correspond to each other [31]].

In the crystal structure, the inverted TTT molecules are arranged in parallel in columns at an angle of 40.2(1)º to the *c* axis, in which they are in contact via π-π interactions [the distance between the molecular planes is 3.426 (1) Å, that between the benzene ring centroids is 3.697 (1) Å] (Figure 4).[26] Dispersive interactions between any one column and the four neighbouring columns (Figure 4S, Supplementary material) stabilize the crystal lattice.

From the free energy difference between forms **a** and **e** in methanol, predicted at the MP2/cc-pVDZ(PCM–methanol) level of theory (Table 1), it emerges that TTT should co-exist in both tautomeric forms under equilibrium conditions with a small percentage of **e**. This prompted us to carry out spectroscopic investigations to check whether the expected molecules of tautomer **e** could be monitored. The results of electronic, infrared and NMR absorption measurements are shown in Table 3. Two bands in the UV spectra of TTT, whose position and intensity depend only slightly on solvent features, may be due, as in other acetyl benzene-1,3,5-triols, to $n\pi^*$ (long wavelength) and $\pi\pi^*$ (short wavelength) transitions.[4] The wavenumber of the C=O stretching vibration in TTT is weakly shifted toward higher values when solvent polarity increases. There are only two signals in the $^1$H NMR spectrum of TTT – a singlet at high field corresponding to the H atoms of $CH_3$ and a diffuse singlet at a very low field assigned to the H atoms of –OH. This latter signal is distinctly shifted toward the low field relative to that in BT,[32] which may be due to the electron-withdrawing effect of the acetyl substituents and the involvement of these and –OH in intramolecular H-bonds. In the $^{13}$C NMR spectrum of TTT in $CDCl_3$, four signals are seen at (values in ppm, numbering of C atoms – Figure 3): 205 [corresponding to C8, C10, and C12 (C=O)], 176 [corresponding to C1, C3 and C5 (C–OH)], 103 [corresponding to C2, C4 and C6 (C-acetyl)] and 33 [corresponding to C13, C15 and C17 ($CH_3$)]; some of these signals correspond well to those found in the $^{13}$C NMR spectra of 1-(2-hydroxy-6-methoxyphenyl)ethanone and 1-(2,6-

dimethoxyphenyl)ethanone.[32] Therefore, the spectral investigations do not show that forms **a** and **e** of TTT co-exist in solution.

The tautomeric forms **a** and **e** of TTT may be converted into one another by H atom (proton) transfer within intramolecular O–H···O bonds [the existence of such H-bonds is demonstrated both by X-ray investigations (Figure 3) and computations (Table 2S, Supplementary material)]. The free energy barrier to H atom transfer within a single O–H···O bond in **a**, predicted at the MP2/cc-pVDZ(PCM–methanol) level of theory, is only 4.41 kcal/mol [the geometry of H-bonds in the transition state is demonstrated in Figure 1S and Table 2S (Supplementary material)], which facilitates the consecutive transfer of an H atom within three H-bonds and the mutual transformation of **a** into **e** and *vice versa* (the Gibbs' free energy barrier, predicted at the MP2/cc-pVDZ level of theory, is 9.05 kcal/mol). It is thus probable that the tautomeric transformations described above are responsible for the spectral behaviour of TTT in solutions. In the solid phase, only the most stable tautomer **a** is incorporated in the crystal lattice.

To conclude, in contrast to BT, TTT may exist in two tautomeric forms of comparable thermodynamic stability. Moreover, the three intramolecular H-bonds stabilizing the molecular structure in TTT may be sites of fast H-atom (proton) transfer between carbonyl and hydroxy O atoms. The occurrence of such a process could mean that the spectral features of TTT are averaged over the two tautomers. We believe that these unique properties of TTT open up new prospects for investigations and applications of it and its derivatives.

**Acknowledgements**

This study was financed by the State Funds for Scientific Research (grant DS/8220-4-0087-1). The calculations were carried out on computers of the Tri-City Academic Network Computer Centre in Gdansk (TASK).

**Supplementary data**

The Supplementary data (experimental procedures, Figures and Tables) associated with this article can be found in the online version at doi:

Complete X-ray data are available from the Cambridge Crystallographic Data Centre: CCDC 800397.

**References and notes**


1. Klarmann, E. *J. Am. Chem. Soc.* **1926**, *48*, 2358 – 2367.
2. Shriner, R. L.; Kleiderer, E. C. *J. Am. Chem. Soc.* **1929**, *51*, 1267 – 1270.
3. Billman, J. H.; Smith, C. M. *J. Am. Chem. Soc.* **1939**, *61*, 457 – 458.
4. Campbell, T. W.; Coppinger, G. M. *J. Am. Chem. Soc*. **1951**, *73*, 2708 – 2712.
5. Marchand, P. A.; Weller, D. M.; Bonsall, R. F. *J. Agric. Food Chem.* **2000**, *48*, 1882 – 1887.
6. Ciochina, R.; Grossman, R. B. *Chem. Rev.* **2006**, *106*, 3963 – 3986.
7. Bowden, K.; Broadbent, J. L.; Ross, W. J. *Brit. J. Pharmacol.* **1965**, *24*, 714 – 724.
8. Kol'tsov, A. I.; Kheifets, G. M. *Russ. Chem. Rev*. **1971**, *40*, 773 – 788.
9. Rubinov, D. B.; Rubinova, I. L.; Akhrem, A. A. *Chem. Natural Comp.* **1995**, *31*, 537 – 559.
10. Singh, I. P.; Sidana, J.; Bharate, S. B.; Foley, W. J. *Nat. Prod. Rep.* **2010**, *27*, 393 – 416.
11. Chong, J. H.; Sauer, M.; Patrick, B. O.; MacLachlan, M. J. *Org. Lett.* **2003**, *5*, 3823 – 3826.
12. Li, Y.; Lampkins, A. J.; Baker, M. B.; Sumpter, B. G.; Huang, J.; Abboud, K. A.; Castellano, R. K. *Org. Lett.* **2009**, *11*, 4314 – 4317.
13. Highet, R. J.; Ekhato, I. V. *J. Org. Chem*. **1988**, *53*, 2843 – 2844.
14. Lohrie, M.; Knoche, W. *J. Am. Chem. Soc*. **1993**, *115*, 919 – 924.
15. Fiege, H.; Voges, H.-W.; Hamamoto, T.; Umemura, S.; Iwata, T.; Miki, H.; Fujita, Y.; Buysch, H.-J.; Garbe, D.; Paulus, W. In: *Ullmann's Encyclopedia of Industrial Chemistry: Phenol Derivatives*; Wiley-VCH: Weinheim, 2000; Vol. 19A (revised), pp 313 – 369.
16. Nishiya, T.; Yamauchi, S.; Hirota, N.; Baba, M.; Hanazaki, I. *J. Phys. Chem*. **1986**, *90*, 5730 – 5735.
17. Harcourt, M. P.; O'Ferrall, R. A. M. *J. Chem. Soc., Perkin Trans. 2* **1995**, 1415 – 1425.
18. Chiang, Y.; Kresge, A. J.; Wirz, J. *J. Am. Chem. Soc.* **1984**, *106*, 6392 – 6395.
19. Møller, C.; Plesset, M. S. *Phys. Rev.* **1934**, *46*, 618 – 622.
20. Davidson, E.; Feller, D. *Chem. Rev*. **1986**, *86*, 681 – 696.
21. Dunning, T. H. *J. Chem. Phys.* **1989**, *90*, 1007 – 1023.
22. Frisch, M. J.; Trucks, G. W.; Schlegel, H. B.; Scuseria, G. E.; Robb, M. A.; Cheeseman, J. R.; Montgomery, J. A.; Vreven, T.; Kudin, K. N.; Burant, J. C.; Millam, J. M.; Iyengar, S. S.; Tomasi, J.; Barone, V.; Mennucci, B.; Cossi, M.; Scalmani, G.; Rega, N.; Petersson, G. A.; Nakatsuji, H.; Hada, M.; Ehara, M.; Toyota, K.; Fukuda, R.;

Hasegawa, J.; Ishida, M.; Nakajima, T.; Honda, Y.; Kitao, O.; Nakai, H.; Klene, M.; Li, X.; Knox, J. E.; Hratchian, H. P.; Cross, J. B.; Bakken, V.; Adamo, C.; Jaramillo, J.; Gomperts, R.; Stratmann, R. E.; Yazyev, O.; Austin, A. J.; Cammi, R.; Pomelli, C.; Ochterski, J. W.; Ayala, P. Y.; Morokuma, K.; Voth, G. A.; Salvador, P.; Dannenberg, J. J.; Zakrzewski, V. G.; Dapprich, S.; Daniels, A. D.; Strain, M. C.; Farkas, O.; Malick, D. K.; Rabuck, A. D.; Raghavachari, K.; Foresman, J. B.; Ortiz, J. V.; Cui, Q.; Baboul, A. G.; Clifford, S.; Cioslowski, J.; Stefanov, B. B.; Liu, G.; Liashenko, A.; Piskorz, P.; Komaromi, I.; Martin, R. L.; Fox, D. J.; Keith, T.; Al-Laham, M. A.; Peng, C. Y.; Nanayakkara, A.; Challacombe, M.; Gill, P. M. W.; Johnson, B.; Chen, W.; Wong, M. W.; Gonzalez, C.; Pople, J. A. *Gaussian 03*, revision C.02; Gaussian, Inc.: Wallingford, CT, 2004.

23. Tomasi, J.; Persico, M. *Chem. Rev.* **1994**, *94*, 2027 – 2094.
24. Barone, V.; Cossi, M.; Mennucci, B.; Tomasi. J. *J. Chem. Phys.* **1997**, *107*, 3210 – 3221.
25. Aakeröy, C. B.; Seddon, K. R.; Leslie, M. *Struct. Chem*. **1992**, *3*, 63 – 65.
26. Hunter, C. A.; Lawson, K. R.; Perkins, J.; Urch, C. J. *J. Chem. Soc., Perkin Trans. 2* **2001**, 651 – 669.
27. Maartmann-Moe, K. *Acta Crystallogr.* **1965**, *19*, 155 – 157.
28. Tanimoto, Y.; Kobayashi, H.; Nagakura, S.; Saito, Y. *Acta Crystallogr., Sect B* **1973**, *29*, 1822 – 1826.
29. Friščić, T.; Drab, D. M.; MacGillivray, L. R. *Org. Lett.* **2004**, *6*, 4647 – 4650.
30. Budzianowski, A.; Katrusiak, A. *Acta Crystallogr., Sect. B* **2006**, *62*, 94–101.
31. Boyer, D. G.; Boisdon, M.-T.; Rochal, A.; Munoz, A. *Phosphorus, Sulfur, Silicon* **2003**, *178*, 2117 – 2125.
32. Mandix, K.; Colding, A.; Elming, K.; Sunesen, L.; Shim I. *Int. J. Quant. Chem.* **1993**, *46*, 159 – 170.

**Table 1** Thermodynamic data for the TTT tautomers.[a]

| Tautomer | Gaseous phase | | Methanol | |
|---|---|---|---|---|
| | $\Delta G$ | $x$ | $\Delta G$ | $x$ |
| **a** | | 1.000 | | 0.975 |
| **b** | 29.2 | | 29.6 | |
| **c** | 69.9 | | 66.0 | |
| **d** | 84.3 | | 89.6 | |
| **e** | 5.97 | | 2.18 | 0.025 |

[a] Values obtained at the MP2/cc-pVDZ level of theory (gaseous phase) or MP2/cc-pVDZ(PCM–methanol) level of theory (methanolic phase); $\Delta G$ – Gibbs' free energy of a given tautomer relative to the Gibbs' free energy of tautomer **a** (Figure 1), equal to (in Hartree) – 913.197382 (gaseous phase), or free energy of a given tautomer relative to the free energy of tautomer **a**, equal to (in Hartree) – 915.786577 (methanolic phase), at 298.14 K (in kcal/mol); $x$ – mole fraction of a given tautomer under equilibrium conditions.

**Table 2** Structural characteristics of tautomers **a** and **e** of TTT, molecule **a'** and the transition state corresponding to H-atom transfer within a single intramolecular H-bond in **a** (**t**).

| Entity | Method[a] | A[b] | Molecular geometry[c] | | | | H-bond geometry | | |
|---|---|---|---|---|---|---|---|---|---|
| | | | C–O | C=O | C–C (r–r) | C–C (r–s) | O–H | H···O | O–H···O |
| **a** | MP2 | 0.0 | 1.328 | 1.252 | 1.426 | 1.479 | 1.020[d] | 1.485[d] | 156[d] |
| **a** | X-ray | 0.060 (1) | 1.323 | 1.257 | 1.416 | 1.465 | 0.99[d] | 1.48[d] | 159[d] |
| **e** | MP2 | 0.0 | 1.304 | 1.272 | 1.459 | 1.414 | 1.057[d] | 1.398[d] | 158[d] |
| **a'** | MP2 | 0.26 | 1.348 | 1.216 | 1.416 | 1.503 | 0.966 | | |
| **t** | MP2 | 0.0 | 1.314 | 1.263 | 1.427 | 1.465 | 1.178[e] | 1.293[e] | 149[e] |

[a] MP2 – the MP2/cc-pVDZ(PCM–methanol) level of theory.
[b] A – average deviation from planarity of the molecular system involving all C and O atoms.
[c] Mean lengths of C–O, C=O, C–C (ring–ring) and C–C (ring–substituent) bonds (in Å).
[d] Geometry of intramolecular hydrogen bonds: O–H (mean length in Å), H···O (mean distance in Å), O–H···O (mean angle in deg) (details in Table 2S, Supplementary material).
[e] Geometry of an H-bond involved in H-atom transfer (details in Table 2S, Supplementary material).

**Table 3** Electronic, infrared and $^1$H NMR absorption data for TTT dissolved in various solvents.[a]

| Medium | $^1$H NMR | | | IR | | Electronic absorption | | |
|---|---|---|---|---|---|---|---|---|
| | solvent | $\delta_H$ (OH) | $\delta_H$ ($CH_3$) | solvent | $\nu_{C=O}$ | solvent | $\lambda_{max}$ | *lg* ε |
| non-polar | $CDCl_3$ | 17.18 (1H) | 2.72 (9H) | $CCl_4$ | 1622 | hexane | 324 (nπ*)<br>266 (ππ*) | 3.68<br>4.83 |
| polar | DMSO–$d_6$ | 17.21 (1H) | 3.31 (9H) | $CH_3CN$ | 1628 | $CH_3OH$ | 325 (nπ*)<br>266 (ππ*) | 3.62<br>4.79 |

[a] $\delta_H$ – chemical shift of H atoms in ppm; $\nu_{C=O}$ – wavenumber of the C=O stretching vibration in $cm^{-1}$; $\lambda_{max}$ – wavelength of the band maxima in UV spectra in nm; ε –molar absorption coefficient; nπ* and ππ* – types of electronic transition.

**Figure Captions**

Figure 1. Canonical structures of the possible tautomeric forms of TTT.

Figure 2. Types of keto/enol tautomerism exhibited in TTT.

Figure 3. ORTEP view of the crystal structure of the TTT molecule (dashed lines represent H-bonds).

Figure 4. Packing of TTT molecules in the crystal (H-bonds are represented by dashed lines, π–π interactions by dotted lines).

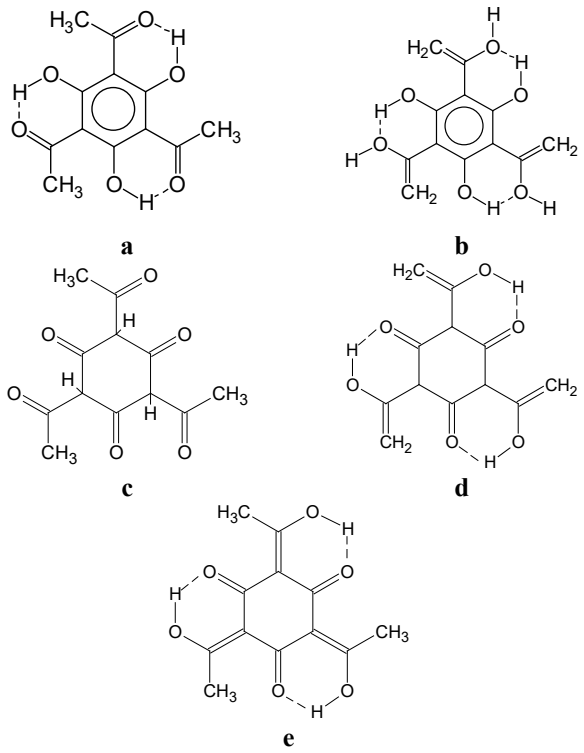


**Figure 1.**

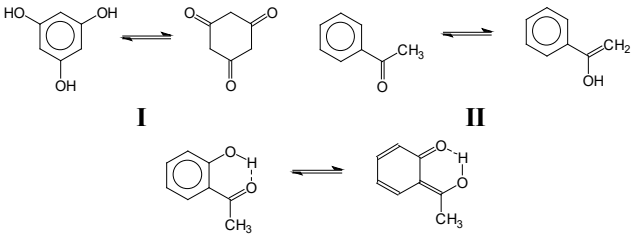


**Figure 2.**

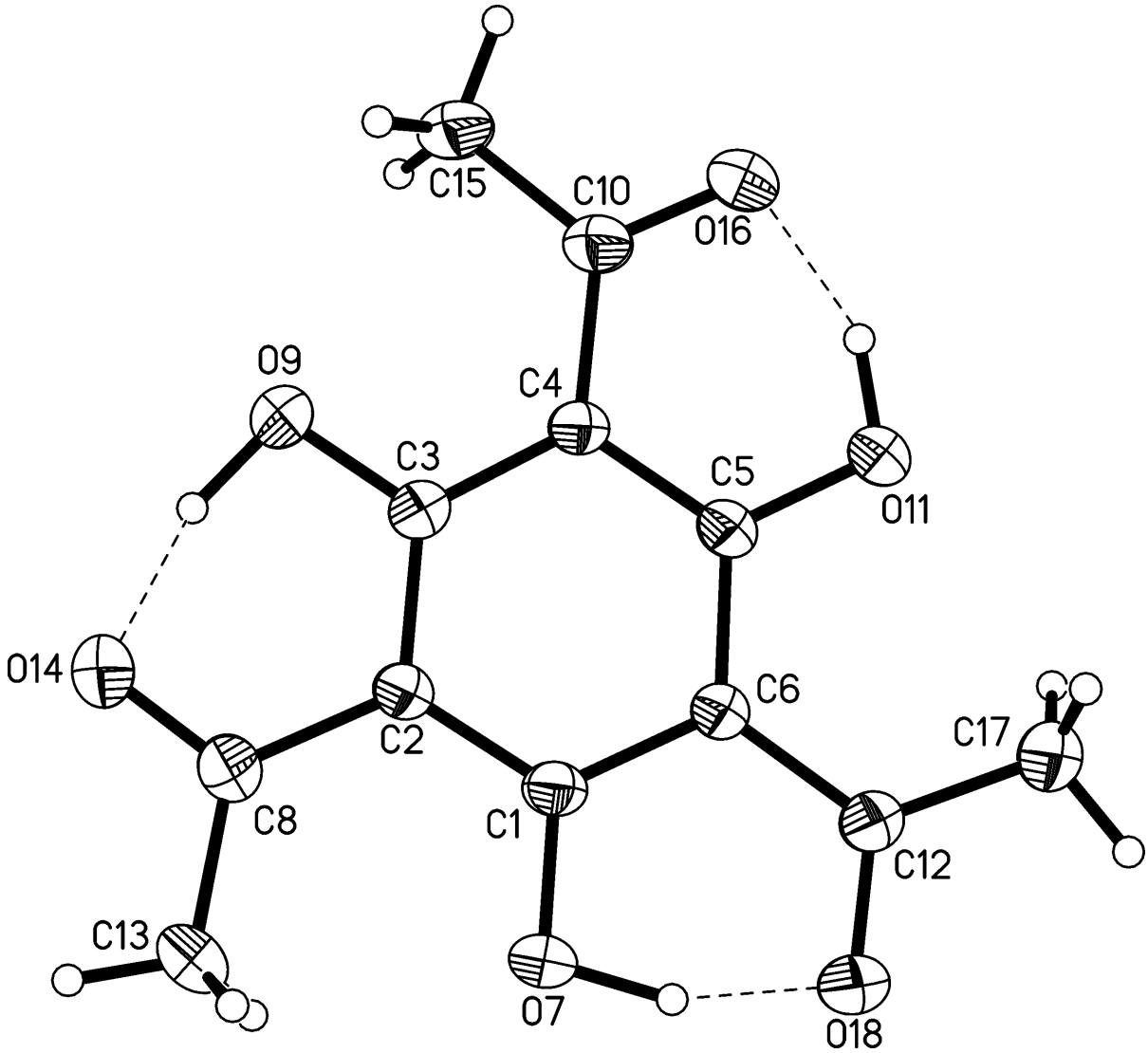


**Figure 3.**

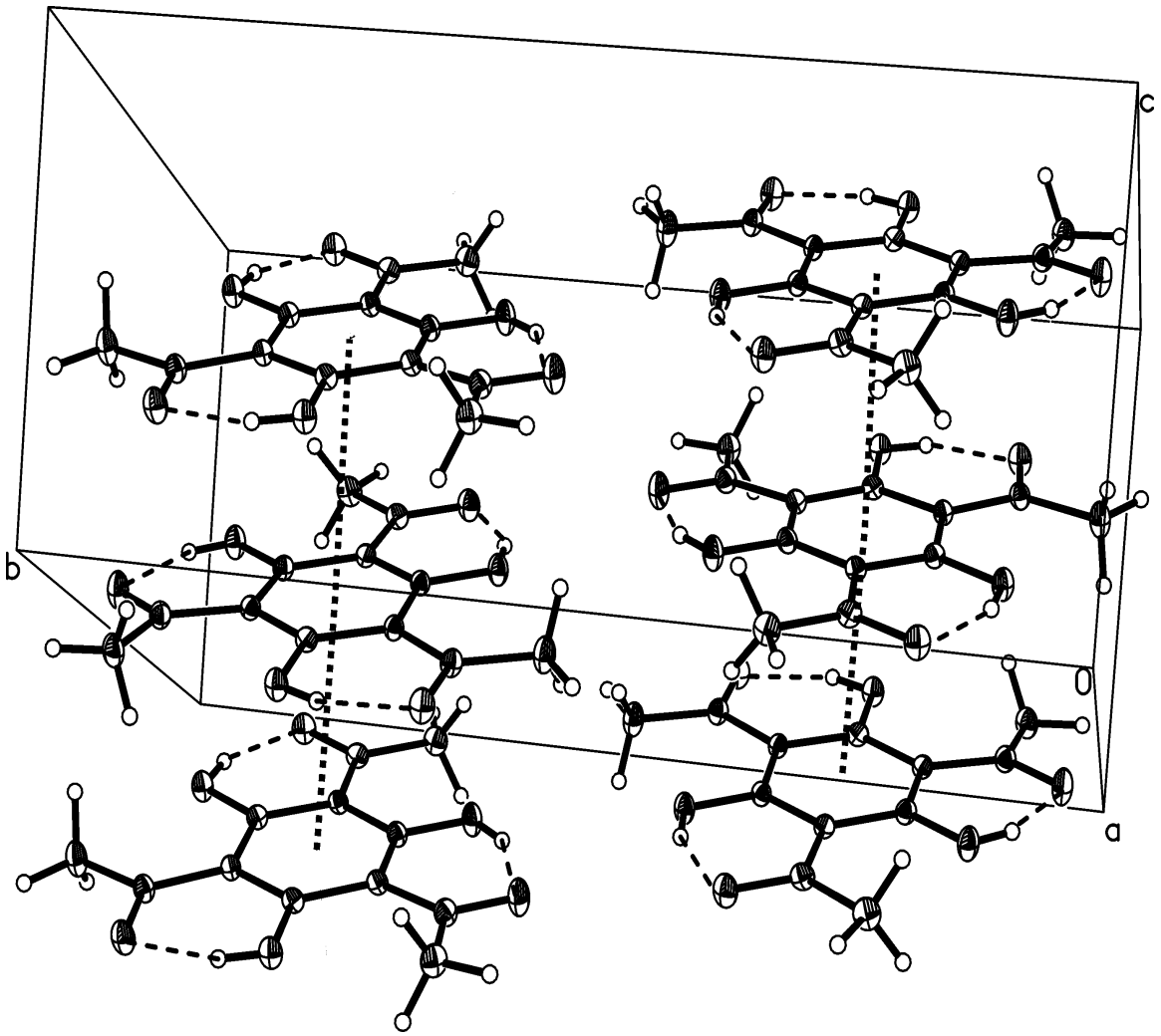


**Figure 4.**